

AD-A190 947

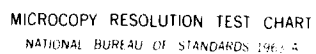
STUDIES OF IONOSPHERE/MAGNETOSPHERE DYNAMICS USING  
SABRE AND HILAT(U) LEICESTER UNIV (ENGLAND) DEPT OF  
PHYSICS I A JONES ET AL. 28 SEP 87 AFGL-TR-87-8273  
AFOSR-84-0077 P/G 4/1

1/1

UNCLASSIFIED

ML

END  
DATE  
FILMED  
58



MICROCOPY RESOLUTION TEST CHART  
NATIONAL BUREAU OF STANDARDS 1963-A

DTIC FILE COPY

④

AD-A190 947

AD-A190 947  
AD-A190 947

T. B. Jones  
J. A. Haddock

University of Leicester  
Department of Physics  
University Road  
Leicester, LE1 7RH, U.K.

20 September 1987

Final Report  
1 March 1986-28 February 1987

APPROVED FOR PUBLIC RELEASE; DISTRIBUTION UNLIMITED

DTIC  
ELECTE  
MAR 02 1988

S D

AD-A190 947

AD-A190 947

AD-A190 947

"This technical report has been reviewed and is approved for publication"

*John A. K. Kuchel*

JOHN A. K. KUCHEL  
Contract Manager  
Ionospheric Effects Branch

*H. C. Carlson*

HERBERT C. CARLSON  
Ionospheric Effects Branch  
Ionospheric Physics Division

FOR THE COMMANDER

*R. J. Krivanek*

ROBERT J. KRIVANEK  
Director  
Ionospheric Physics Division

This report has been reviewed by the ESD Public Affairs Office (PA) and is releasable to the National Technical Information Service (NTIS).

Qualified requestors may obtain additional copies from the Defense Technical Information Center. All others should apply to the National Technical Information Service.

If your address has changed, or if you wish to be removed from the mailing list, or if the addressee is no longer employed by your organization, please notify AFGL/DAA, Hanscom AFB, MA 01731. This will assist us in maintaining a current mailing list.

Do not return copies of this report unless contractual obligations or notices on a specific document require that it be returned.

UNCLASSIFIED  
SECURITY CLASSIFICATION OF THIS PAGE

REPORT DOCUMENTATION PAGE				Form Approved OMB No. 0704-0188	
1a. REPORT SECURITY CLASSIFICATION UNCLASSIFIED			1b. RESTRICTIVE MARKINGS <b>AD-A190 947</b>		
2a. SECURITY CLASSIFICATION AUTHORITY			3. DISTRIBUTION/AVAILABILITY OF REPORT APPROVED FOR PUBLIC RELEASE, DISTRIBUTION UNLIMITED.		
2b. DECLASSIFICATION/DOWNGRADING SCHEDULE					
4. PERFORMING ORGANIZATION REPORT NUMBER(S) AFOSR-84-0077-2			5. MONITORING ORGANIZATION REPORT NUMBER(S) AFGL-TR-87-0273		
6a. NAME OF PERFORMING ORGANIZATION UNIVERSITY OF LEICESTER		6b. OFFICE SYMBOL (If applicable)		7a. NAME OF MONITORING ORGANIZATION EOARD	
6c. ADDRESS (City, State, and ZIP Code) DEPARTMENT OF PHYSICS, UNIVERISTY OF LEICESTER, UNIVERSITY ROAD, LEICESTER, LE17RH, U.K.			7b. ADDRESS (City, State, and ZIP Code) 223/231 OLD MARYLEBONE ROAD, LONDON, NW1 5TH.		
8a. NAME OF FUNDING/SPONSORING ORGANIZATION AIR FORCE GEOPHYSICS LABORATORY		8b. OFFICE SYMBOL (If applicable)		9. PROCUREMENT INSTRUMENT IDENTIFICATION NUMBER AFOSR-84-0077	
8c. ADDRESS (City, State, and ZIP Code) HANSCOM AFB, MASSACHUSETTS, 01731, U.S.A.			10. SOURCE OF FUNDING NUMBERS		
			PROGRAM ELEMENT NO. 62101F	PROJECT NO. 4643	TASK NO. 09
			WORK UNIT ACCESSION NO. AF		
11. TITLE (Include Security Classification) STUDIES OF IONOSPHERE/MAGNETOSPHERE DYNAMICS USING SABRE AND HILAT (UNCLASSIFIED)					
12. PERSONAL AUTHOR(S) JONES, TUDOR, BOWDEN; WALDOCK, JEFFREY, ANDREW.					
13a. TYPE OF REPORT FINAL		13b. TIME COVERED FROM MAR 86 TO 28 FEB 87		14. DATE OF REPORT (Year, Month, Day) 1987 September 20	
15. PAGE COUNT 26					
16. SUPPLEMENTARY NOTATION					
17. COSATI CODES			18. SUBJECT TERMS (Continue on reverse if necessary and identify by block number)		
FIELD	GROUP	SUB-GROUP	SABRE, HILAT, AURORAL BACKSCATTER, IRREGULARITIES, CONVECTION, ASPECT ANGLE ATTENUATION, IMF.		
19. ABSTRACT (Continue on reverse if necessary and identify by block number) Plasma drifts measured by SABRE in the E-region have been compared with those obtained from HILAT, at an altitude of 800 km, during a pass on March 1 1984. Results are not consistent with perfect mapping of the electric field between the two regions. Furthermore, no field-aligned current signature is observed by SABRE. A comparison of E-region plasma drifts measured by SABRE and F-region scintillations measured by the NNSS satellites suggests that the latter may be related to regions of reduced electric field in the F-region. This is consistent with the presence of field-aligned currents which produce kilometre-scale structure in the F-region plasma. Mean plasma convection patterns in the E-region have been derived as a function of the IMF components By and Bz and the magnetic index Kp. Convection flows are much stronger for southward Bz. The time of the evening convection reversal occurs at later local times for increasingly negative By. As Kp increases radar measurements occur during a higher proportion of the day and the evening convection reversal also moves to earlier local times. Key words:					
20. DISTRIBUTION/AVAILABILITY OF ABSTRACT <input checked="" type="checkbox"/> UNCLASSIFIED/UNLIMITED <input type="checkbox"/> SAME AS RPT. <input type="checkbox"/> DTIC USERS			21. ABSTRACT SECURITY CLASSIFICATION UNCLASSIFIED		
22a. NAME OF RESPONSIBLE INDIVIDUAL John Klobuchar			22b. TELEPHONE (Include Area Code) AFGL/L1S		22c. OFFICE SYMBOL AFGL/L1S

## STUDIES OF IONOSPHERE/MAGNETOSPHERE DYNAMICS USING SABRE AND HILAT

### INTRODUCTION

The scientific objectives of the joint SABRE/HILAT project are designed to provide new insight into the physics of E and F region high latitude plasma irregularities and their dependence on ambient properties of the medium, such as the large-scale density and velocity structure. The plasma gradients associated with these phenomena provide a suitable environment for certain instability processes to generate kilometre-scale irregularities, which are responsible for the scintillation effects which degrade trans-ionospheric UHF communication links. It is therefore important that the generation, transport and decay of these irregularities are more fully understood. This requires measurement of the various irregularity parameters by coordinated multi-technique experiments. One of these is the HILAT satellite, which was launched on June 27 1983, and provides in-situ measurements of scintillation structure and other particle and field data with high time resolution along the track of its orbit. The satellite has a velocity of approximately 7 km/s and hence this data set is effectively a snapshot of the ionosphere along the satellite trajectory. It therefore becomes difficult to separate spatial and temporal variations and the satellite may be unable to resolve the source region, since the irregularities are not static. Consequently it is necessary to coordinate the HILAT measurements with ground-based observations such as those made by the Sweden and Britain Auroral Radar Experiment (SABRE).

SABRE is a bistatic auroral radar experiment, similar to STARE but situated at lower latitudes, covering the L-shell range of approximately 4 to 6. The two radar installations at Wick, in Scotland, and at Uppsala, in Sweden (Figure 1), are operated by Leicester University, UK and by the Max-Planck Institut fur Aeronomie, FRG in cooperation with the Uppsala Ionospheric Observatory. The radars are able to estimate the two dimensional perpendicular electric field within their common field of view (0-12 degrees east, 64-68 degrees north geographic) with a spatial resolution of approximately 20x20 km and a temporal resolution of 20s. During times of special interest, these data are compared with measurements made by the instruments on board the HILAT satellite and with other ground-based facilities in northern Europe, such as EISCAT. The primary scientific objectives of the project are:

1. Irregularity growth rate and decay studies. It is intended to apply the time history of electric field data recorded by the SABRE together with simultaneous HILAT data to test theories of irregularity growth rate, decay rate and accumulative effects (convection of de-stabilized plasma into regions in which the ambient ionospheric conditions inhibit irregularity growth).
2. Investigation of the irregularity dependence on electrostatic turbulence. Spectral analysis of scintillation radio beacon data will be compared with SABRE and HILAT electric fields and velocity shears, together with other measured HILAT parameters.
3. Threshold studies. SABRE and radio beacon data will be compared to examine the scintillation production thresholds in relation to the

plasmopause.

4. Investigation of convection-driven re-distribution of structured plasma. This will involve comparisons of scintillation anisotropies, incoherent scatter electron density profiles and SABRE electric field patterns.

5. Comparison of the spatial and temporal features of the scintillation producing irregularities.

6. Detailed examination of the nature of the high latitude convection flow pattern under different conditions from long-timescale measurements made by SABRE. This will provide a framework within which HILAT data may be interpreted.

#### SABRE/HILAT COMPARISONS

A number of attempts were made to correlate HILAT measurements with those of the SABRE system. From 1-20 December 1984, a joint SABRE/STARE/HILAT campaign was held. During this period, SABRE was fully-operational and good backscatter was observed during most of the intervals of interest. Unfortunately, due to attitude problems with HILAT, the in-situ ion drift velocities measured by HILAT were unreliable and could not be used for direct comparison with the SABRE drifts. Furthermore, the times during which good E-region measurements were available from SABRE did not coincide with HILAT passes in which either the in-situ position (for particle and drift comparisons) or the F-region intersection of the line-of-sight to the beacon receiver at Tromso (for E-region effects associated with scintillation phenomena) passed across field lines threading the radar viewing area.

During a visit to AFGL in May 1985 a search was made of the HILAT database stored on microfiche. Three possible events were identified, of which just one yielded a good comparison. This event was on March 1, 1984 (day 61) between 23:17 and 23:19 UT during a southward bound pass by HILAT. The ground track of the satellite is illustrated in Figure 2. The data recorded by HILAT are illustrated in Figures 3a and b, in which the vertical lines indicate the interval during which the satellite was over the SABRE viewing area. Figure 3a shows ion density, the Tromso S4 index at 137 MHz, the total ion number flux or integral ion flux in particles/(cm ster sec), JTOT, the integral ion energy flux in keV/(cm ster sec), JETOT, and the average ion energy, EAVE, in keV, where EAVE is the ratio of JETOT to JTOT. Figure 3b shows the horizontal and vertical ion velocities measured by ion driftmeters, the RPA measured ion drift velocity together with the Tromso S4 index, which is plotted again for reference.

The ion densities (Figure 3a, lower panel) are high and significant precipitation is taking place, with the average ion energy in the range 1 to 10 keV. The scintillation amplitudes, as indicated by the Tromso S4 index, start to rise at 23:17 UT, reaching saturation level around 23:18 UT. The horizontal ion drift (Figure 3b, top panel) indicates a basically eastward convection velocity (negative value) at this time. The velocity data are compared in detail with SABRE measurements in Figure 4a and b. The auroral radar data, indicated by the horizontal lines, also suggest that the drift is basically eastwards, agreeing in broad detail with HILAT. The HILAT data have a much greater temporal resolution than those from SABRE, but the SABRE

east-west velocity component does not appear to represent an average over 20s of the HILAT measurements. Furthermore, as illustrated in Figure 4b, HILAT measures a significant northward velocity component, which is almost undetected by SABRE. The magnitude of the drift velocity measured by the auroral radar is sometimes a poor approximation to that of the electrons and SABRE may underestimate the drift speed by as much as a factor of 2 (e.g. Robinson, 1986), although the directions of the drift are thought to be accurate (e.g. Nielsen and Schlegel, 1983). If these possible sources of error are taken into account, the north-south velocity comparison improves, but the east-west comparison becomes worse. It appears that the assumption of equipotential field lines, down which the perpendicular electric field can be mapped from high altitudes to the E-region is invalid in this case. It might be expected that a non-zero parallel electric field would be associated with the observed precipitation, and that the associated field-aligned current might result in shear flows in the ionosphere. The existence of such shear flows can be investigated using the spatial resolution of SABRE and Figure 5 illustrates the two-dimensional drift velocity patterns measured by the radar from 23:17 to 23:19 UT. Each pattern is averaged over the 20s period ending at the time indicated in the lower left of each panel. However, no shear flows are apparent, an observation which has yet to be explained.

#### SABRE/SCINTILLATION STUDY

Due to the difficulty in locating suitable conjunctions between HILAT passes and SABRE, a suitable study of SABRE and scintillation effects could not be undertaken. Therefore, a search was made of the Naval Navigational Satellite System (NNSS) database, which provides scintillation indices at Kiruna, held by Dr.L.Kersley at the University College of Wales, Aberystwyth, UK.

A number of passes over SABRE were located and Figure 6 illustrates the satellite scintillation data recorded during one such pass. The signal strength is high and strong amplitude and phase scintillations were observed at around 18:41 on August 26, 1985 (Day 238) at an ionospheric latitude at 350 kms of around 67 degrees north. Figure 7 illustrates the SABRE data recorded at this time, as a sequence of spatial plots, each separated by 20s, with the approximate location of the satellite marked by a ringed cross. The most notable feature of these data is that the scintillations are observed when the transmission path (to Kiruna) passes through part of the F-region which maps to a region of the SABRE viewing area in which backscatter is absent, see panels at 18:40:40, 18:41 and 18:41:20 UT. In view of the fact that irregularities are evidently present in adjacent regions, it is likely that this is due to localised precipitation producing an area of enhanced conductivities. This would have the effect of 'shorting' out the electric field in this region and backscatter would be lost. This E-region signature is frequently observed when scintillations are detected in the F-region above and suggests that at these times, a field aligned current exists, producing kilometer-scale structure in the F-region plasma through a mechanism such as the current-convective instability.

For	
AI	<input checked="" type="checkbox"/>
ed	<input type="checkbox"/>
ation	
tion/	
Availability Codes	
Avail and/or	
Special	



A-1



## PLASMA CONVECTION PATTERNS

As a framework for the SABRE/HILAT comparisons the high latitude convection flow patterns were examined under a variety of different conditions. Mean plasma convection patterns have been deduced from long-timescale measurements made by SABRE, and Figure 8 illustrates the mean convection velocity as a function of Kp using 971 days of data in the interval Day 81, 1982 to Day 212, 1986. Several effects are immediately apparent. Firstly, radar measurements exist within a greater proportion of the day during times of higher Kp, indicating that the overall electric fields are greater. Secondly, the time at which the flow reverses in the evening sector, the Harang discontinuity, moves to earlier local times as Kp increases. Also, there are few observations of flow within the cusp, since it rarely penetrates equatorwards to the latitude range covered by the SABRE.

Recent work has investigated the dependence of the convection pattern on the polarity of the interplanetary magnetic field, using hourly averaged data provided by Dr. J. Vette of the National Space Science Data Center. 902 hours of simultaneous SABRE/IMF measurements were available between April 1982 and June 1984. Figure 9 illustrates the SABRE velocities as a function of IMF Bz at 64 degrees north, geomagnetic latitude. There are evidently fewer data at times when Bz is northward, as might be expected since reconnection at the dayside magnetopause, responsible for the large-scale convection within the magnetosphere, is then inhibited. As Bz becomes increasingly negative, the local time of the Harang discontinuity moves to earlier local times and the amplitude of the convection flow increases.

Figure 10 illustrates the variation of the flow pattern with IMF By. The evening reversal appears to occur at later local times as By becomes increasingly negative, although the situation appears rather confused for strongly positive By. In the vicinity of the morning reversal, although data are scarce under all conditions, flows are more frequently observed when By is positive. The effects are more clearly seen in Figures 11 and 12 which illustrate the variation of the SABRE flows at 64 degrees north averaged over all positive and negative values of Bz (Figure 11) and all positive and negative values of By (Figure 12). The amount of data available at each local time are indicated in the centre of each plot, each concentric circle representing 10 data blocks, each of 15 minutes duration. The flows in the vicinity of the morning reversal for positive By are consistent with the predicted existence of a DPY current system in the ionosphere in the post-noon sector (Rostoker, 1980).

## SUMMARY

It has proved difficult to identify times during which HILAT and SABRE data may be directly compared. For one particular event, on March 1, 1984, the HILAT velocity measurements were quite different from those recorded by SABRE and it is presumed that a parallel electric field existed which prevented the direct mapping of the perpendicular electric fields between the two regions.

A comparison of data from SABRE and the NNSS satellites suggests that F-region scintillations may be associated with regions of reduced electric field in the E-region. This would be consistent with the presence of field-aligned currents de-stabilising the F-region plasma.

The mean plasma convection pattern measured by SABRE is found to be well correlated with the direction of the IMF component  $B_z$ , and convection flows are much stronger for negative  $B_z$ . The time of the evening reversal is also related to the value of  $B_y$  and occurs at later local times as  $B_y$  becomes increasingly negative.

#### BIBLIOGRAPHY

M.D.Burrage, J.A.Waldock, T.B.Jones and E.Nielsen  
Joint SABRE and STARE radar auroral observations of the high latitude  
ionospheric convection pattern. *Nature*, 316, 133-5, 1985.

E.Nielsen and K.Schlegel  
A First Comparison of STARE and EISCAT Electron Drift Velocity  
Measurements. *J.G.R.*, 88, 5745-50, 1983.

T.Robinson  
Towards a self-consistent theory of radar aurora, *J. Atmos. Terr.  
Phys.*, 48, 417-422, 1986.

J.A.Waldock, T.B.Jones and E.Nielsen  
Statistics of 1m wavelength plasma irregularities and convection in  
the auroral E-region., *Radio Sci.*, 20, 709-717, 1985.

T.B.Jones, J.A.Waldock, E.C.Thomas, C.P.Stewart, T.R.Robinson  
SABRE radar observations in the auroral ionosphere  
AGARD Conf.Proc., 382, 6.4.1-15, Fairbanks, Alaska, 1985.

J.A.Waldock, L.Kersley, N.Wheadon, T.B.Jones  
E-Region Convection Flows Observed by SABRE Associated with  
Scintillation-Producing Irregularities in the F-region  
In Preparation, 1987.

#### CONFERENCE PRESENTATIONS

J.A.Waldock  
Aspect Dependence of 1m Plasma Irregularities in the Auroral E-region  
Royal Astronomical Society, M.I.S.T meeting, Liverpool, 10-12 April  
1985.

W.A.C.Mier-Jedrzejowicz, D.J.Southwood, M.W.Dunlop, R.P.Rijnbeek,  
M.Six, J.A.Waldock  
AMPTE-UKS Magnetometer Measurements at the Earth's Magnetopause: New  
Insight into Reconnection  
RAS M.I.S.T Meeting, Liverpool, 10-12 April, 1985.

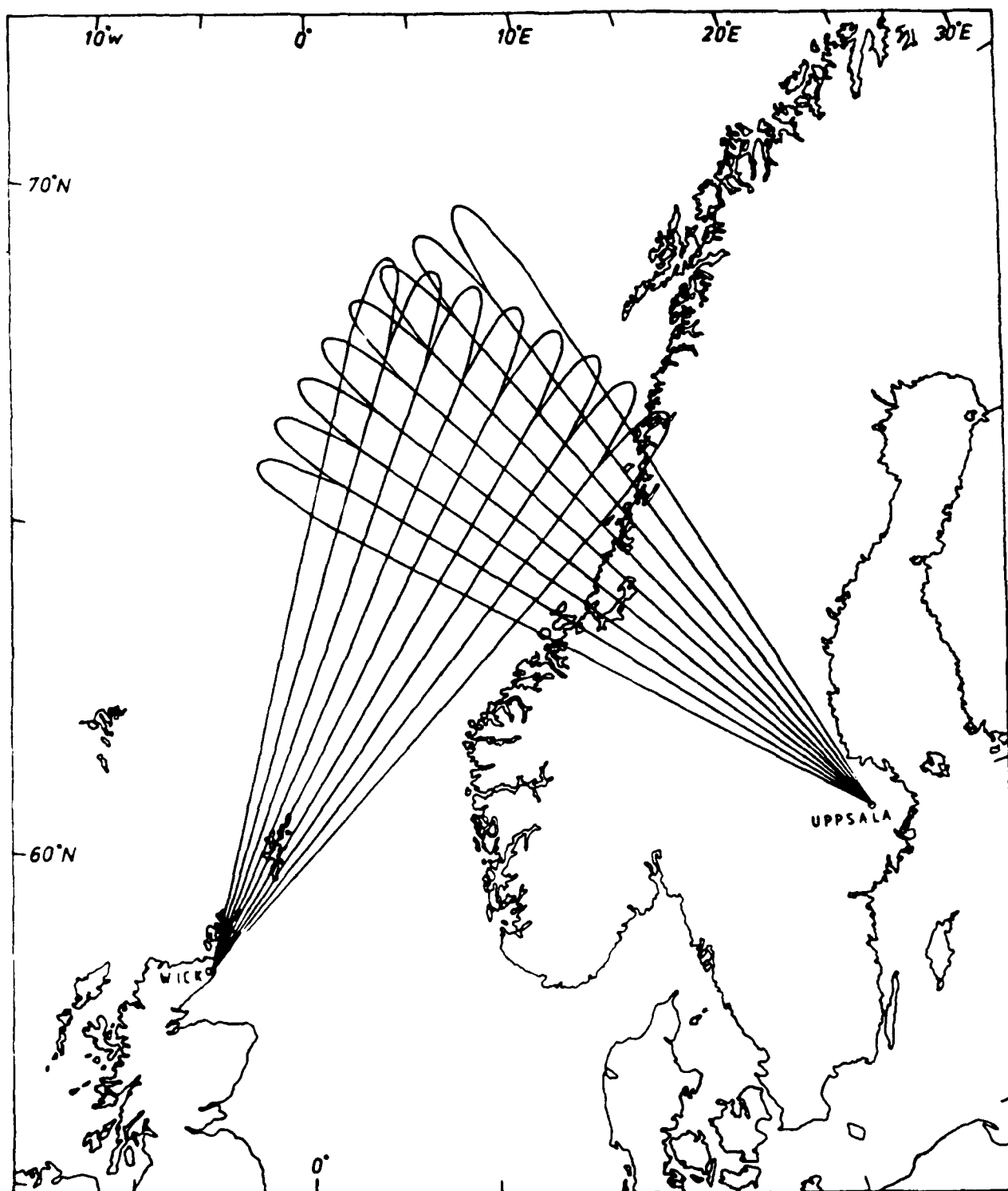
T.R.Robinson and J.A.Waldock  
Studies of Auroral Radar Aspect Angle Scattering  
RAS M.I.S.T Meeting, London, 22 October 1985.

J.A.Waldock and M.D.Burrage  
Interplanetary Magnetic Field effects on the High Latitude Convection  
Pattern.  
RAS M.I.S.T meeting, Edinburgh, 8-9 April 1986.

J.A.Waldock  
Recent Observations of the Radar Aurora Using SABRE  
UK URSI meeting, University of Birmingham, 8-9 July 1986.

#### FIGURE CAPTIONS

- Figure 1. Illustrating the SABRE viewing area.
- Figure 2. The ground track of the HILAT satellite on March 1 1984 during the pass over SABRE
- Figure 3a,b. These figures illustrate the data recorded by HILAT during the event.
- Figure 4a,b. Illustrating the HILAT and SABRE velocity comparisons.
- Figure 5. A sequence of SABRE plots during the HILAT pass.
- Figure 6. Scintillation measurements from NNSS on 26 August 1985
- Figure 7. SABRE data recorded during the pass by NNSS.
- Figure 8. Illustrating the average SABRE convection flows as a function of  $K_p$ .
- Figure 9. Illustrating the average SABRE convection flows as a function of IMF  $B_z$ .
- Figure 10. As figure 9 but for IMF  $B_y$ .
- Figure 11. Illustrating the SABRE convection flows at 64 degrees north for (a)  $B_z < 0$  and (b)  $B_z > 0$  for all  $B_y$ .
- Figure 12. As figure 12 but for  $B_y$ .



Beam Geometry of the Wick and Uppsala Radars

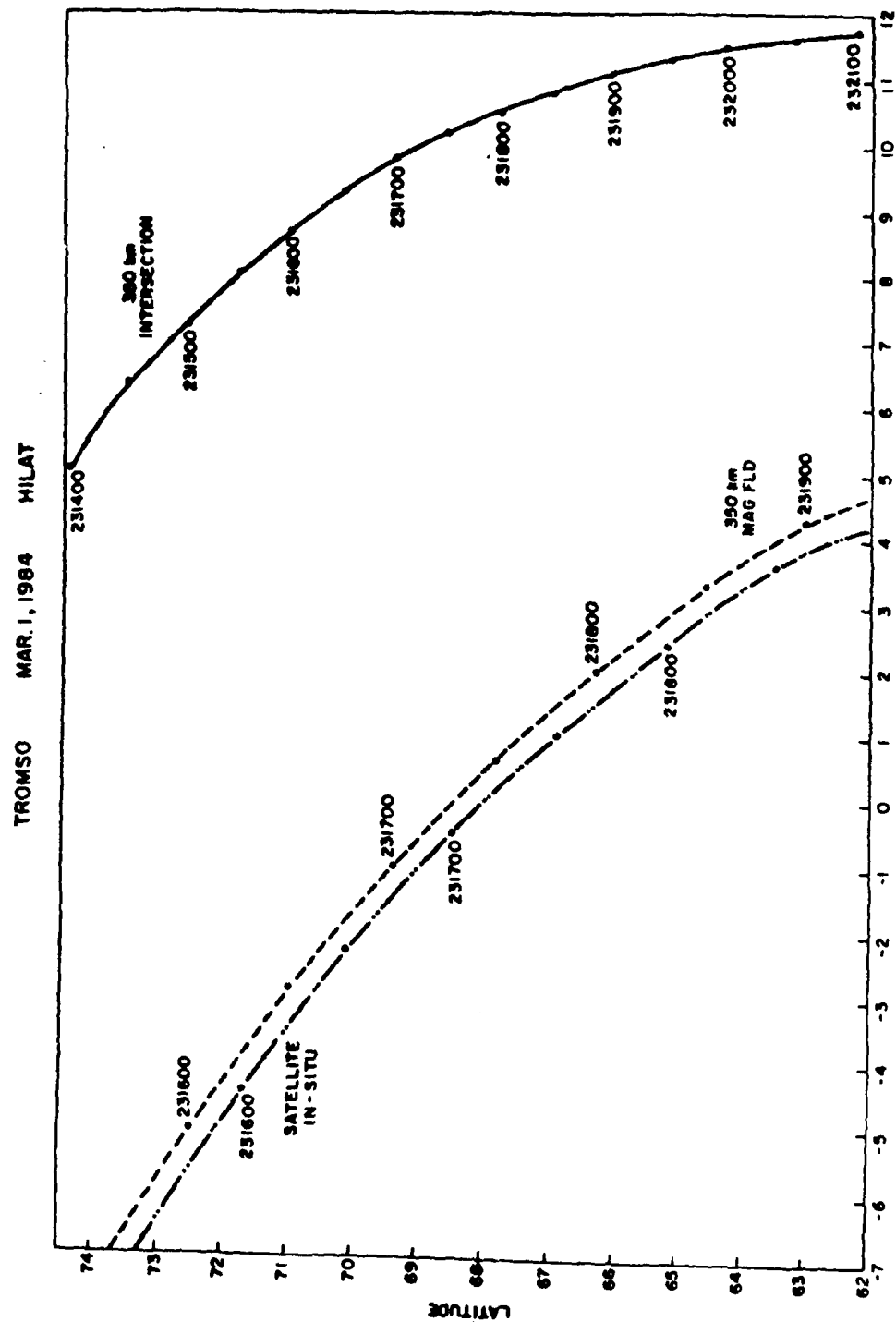
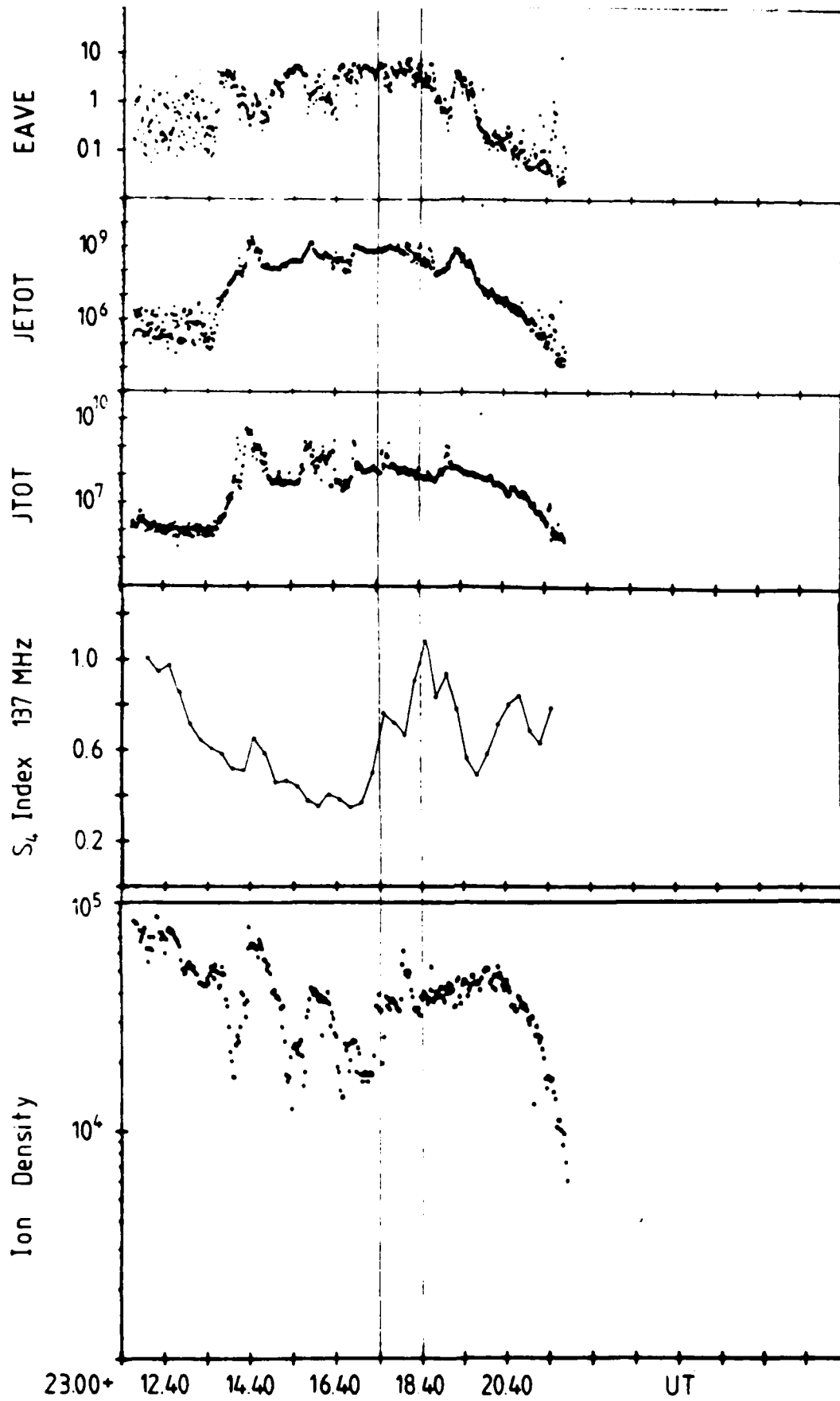


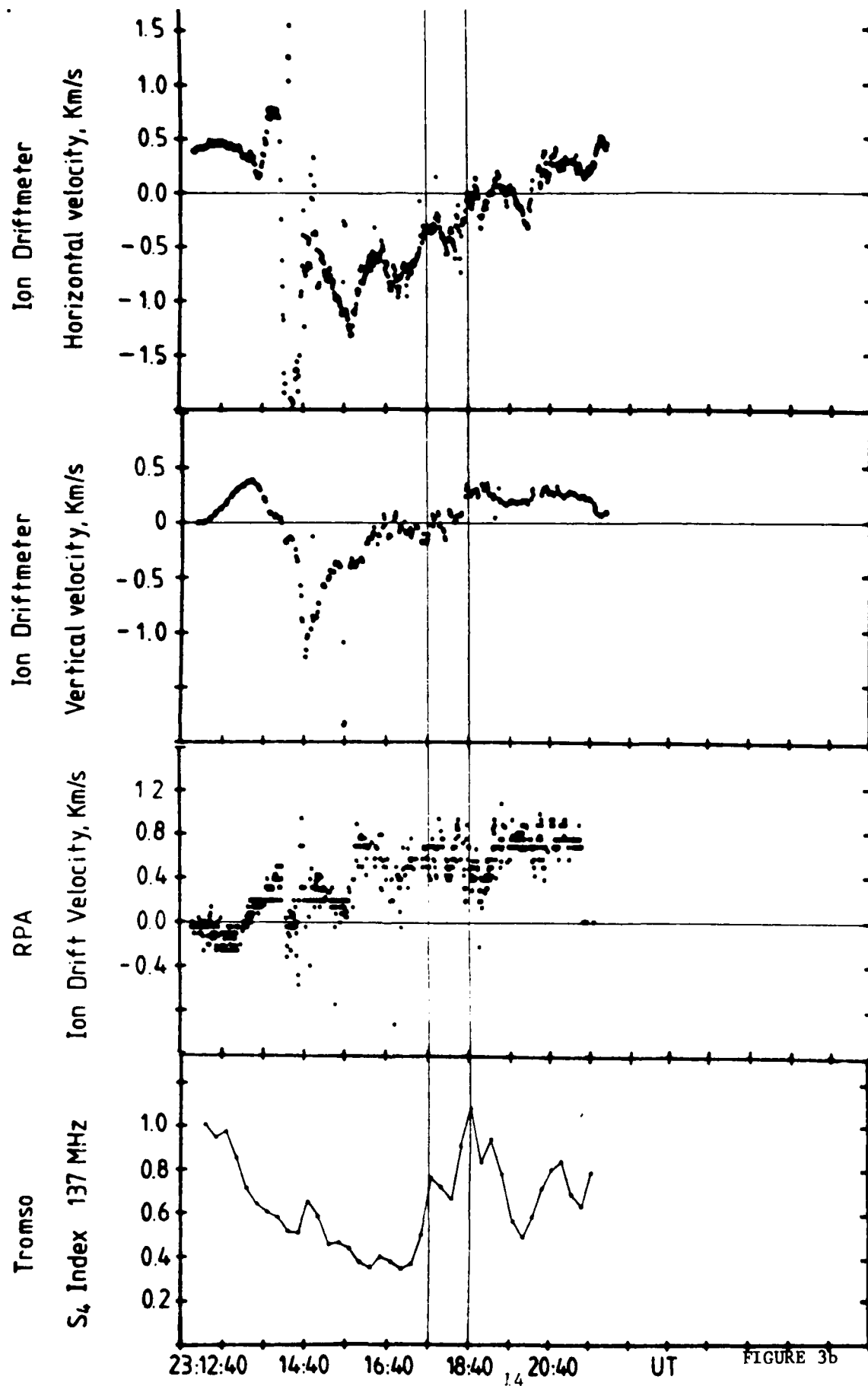
Figure 2



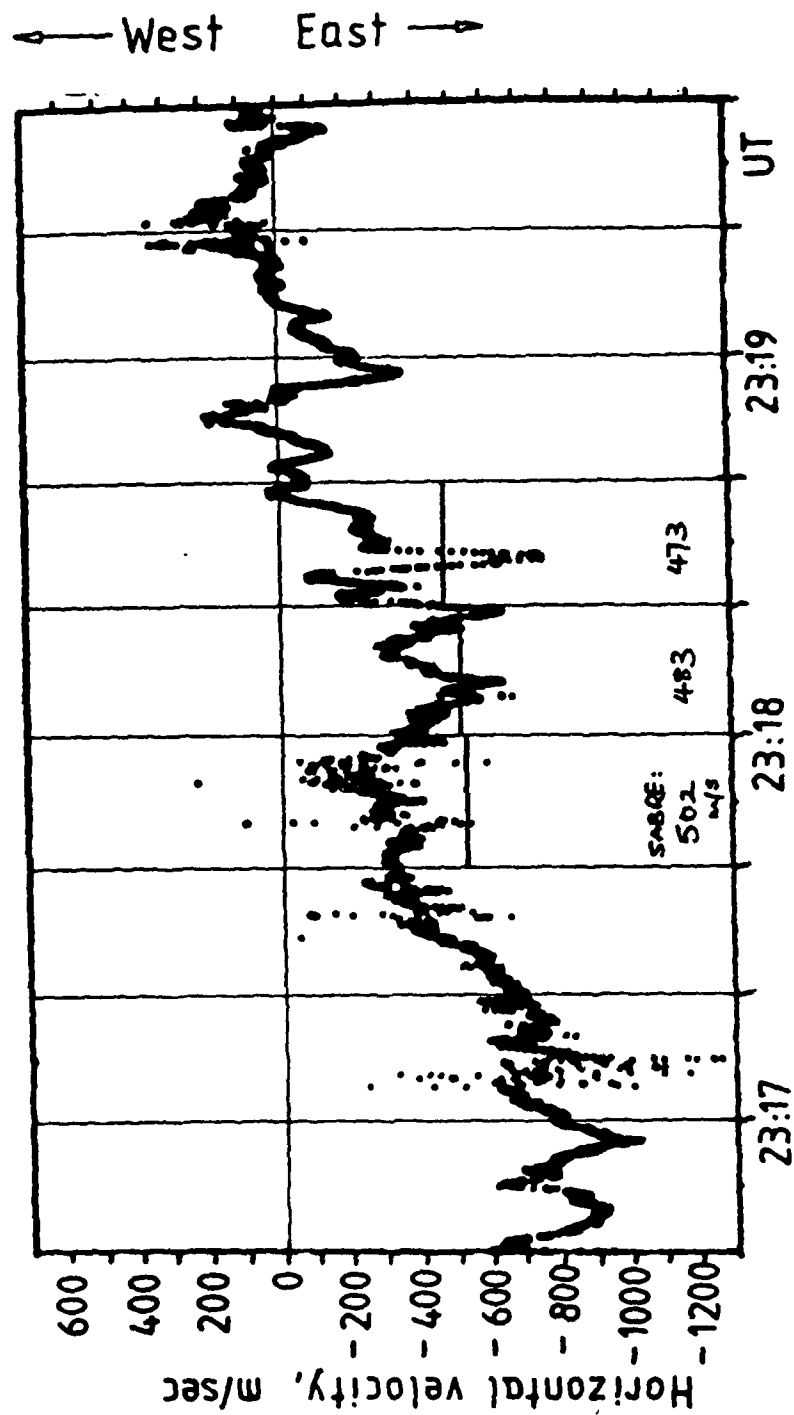
HILAT

Day 61 1984

Figure 3a







HILAT Day 61 1984

Figure 4a

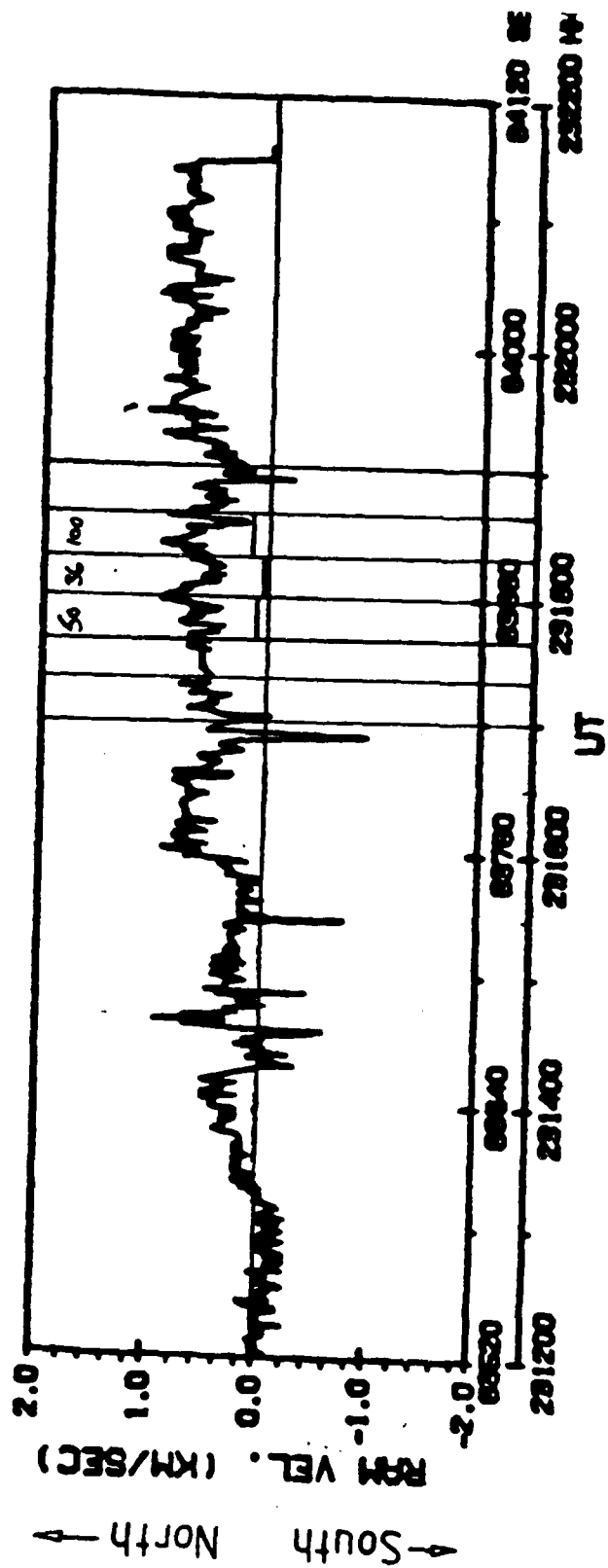
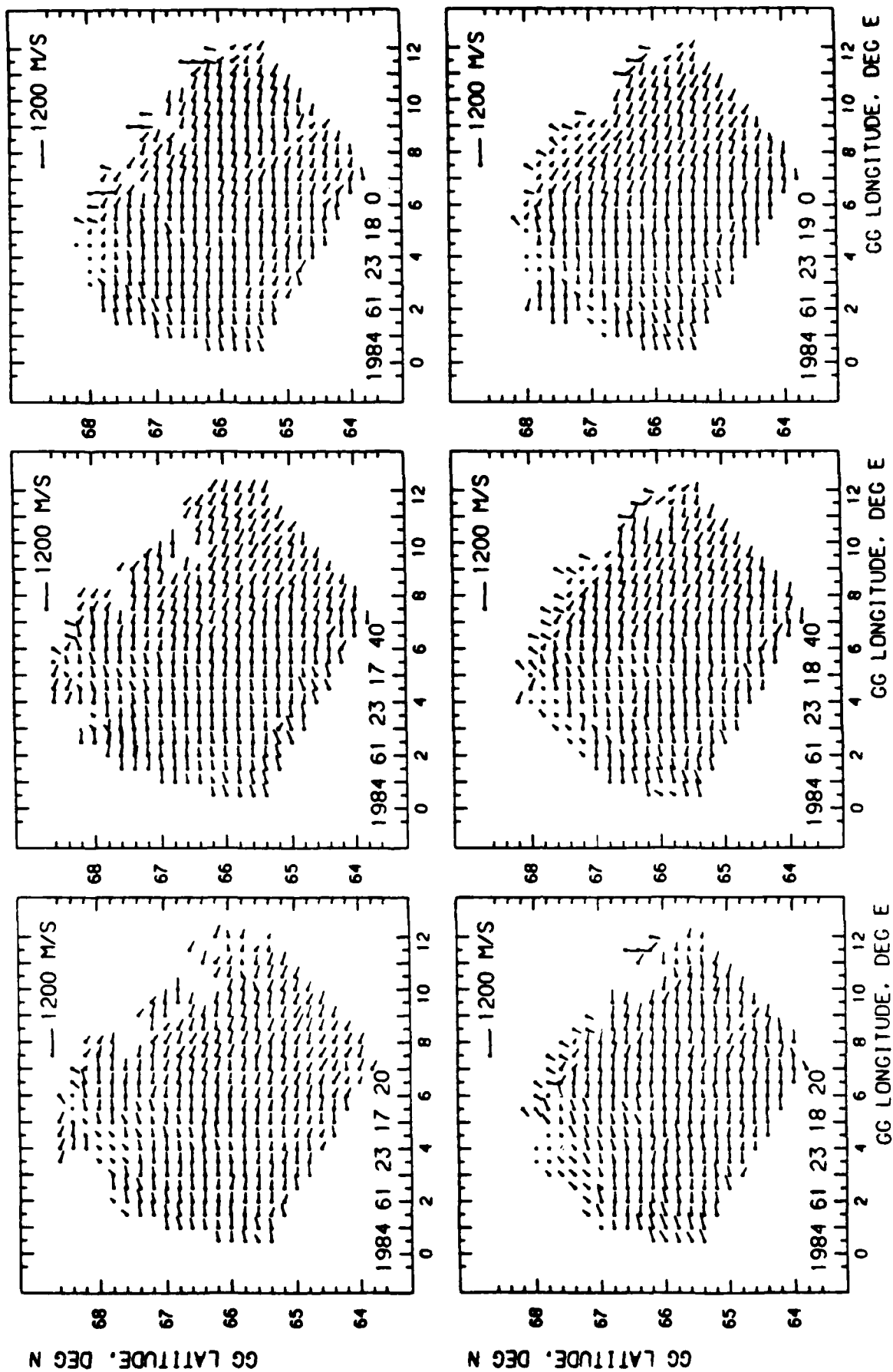
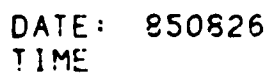


Figure 4b

# SABRE IRREGULARITY DRIFT VELOCITIES





1  
2  
3  
4  
5  
6  
7  
8  
9  
10  
11  
12  
13  
14  
15  
16  
17  
18  
19  
20  
21  
22  
23  
24  
25  
26  
27  
28  
29  
30  
31  
32  
33  
34  
35  
36  
37  
38  
39  
40  
41  
42  
43  
44  
45  
46  
47  
48  
49  
50  
51  
52  
53  
54  
55  
56  
57  
58  
59  
60  
61  
62  
63  
64  
65  
66  
67  
68  
69  
70  
71  
72  
73  
74  
75  
76  
77  
78  
79  
80  
81  
82  
83  
84  
85  
86  
87  
88  
89  
90  
91  
92  
93  
94  
95  
96  
97  
98  
99  
100  
101  
102  
103  
104  
105  
106  
107  
108  
109  
110  
111  
112  
113  
114  
115  
116  
117  
118  
119  
120  
121  
122  
123  
124  
125  
126  
127  
128  
129  
130  
131  
132  
133  
134  
135  
136  
137  
138  
139  
140  
141  
142  
143  
144  
145  
146  
147  
148  
149  
150  
151  
152  
153  
154  
155  
156  
157  
158  
159  
160  
161  
162  
163  
164  
165  
166  
167  
168  
169  
170  
171  
172  
173  
174  
175  
176  
177  
178  
179  
180  
181  
182  
183  
184  
185  
186  
187  
188  
189  
190  
191  
192  
193  
194  
195  
196  
197  
198  
199  
200  
201  
202  
203  
204  
205  
206  
207  
208  
209  
210  
211  
212  
213  
214  
215  
216  
217  
218  
219  
220  
221  
222  
223  
224  
225  
226  
227  
228  
229  
230  
231  
232  
233  
234  
235  
236  
237  
238  
239  
240  
241  
242  
243  
244  
245  
246  
247  
248  
249  
250  
251  
252  
253  
254  
255  
256  
257  
258  
259  
260  
261  
262  
263  
264  
265  
266  
267  
268  
269  
270  
271  
272  
273  
274  
275  
276  
277  
278  
279  
280  
281  
282  
283  
284  
285  
286  
287  
288  
289  
290  
291  
292  
293  
294  
295  
296  
297  
298  
299  
300  
301  
302  
303  
304  
305  
306  
307  
308  
309  
310  
311  
312  
313  
314  
315  
316  
317  
318  
319  
320  
321  
322  
323  
324  
325  
326  
327  
328  
329  
330  
331  
332  
333  
334  
335  
336  
337  
338  
339  
340  
341  
342  
343  
344  
345  
346  
347  
348  
349  
350  
351  
352  
353  
354  
355  
356  
357  
358  
359  
360  
361  
362  
363  
364  
365  
366  
367  
368  
369  
370  
371  
372  
373  
374  
375  
376  
377  
378  
379  
380  
381  
382  
383  
384  
385  
386  
387  
388  
389  
390  
391  
392  
393  
394  
395  
396  
397  
398  
399  
400  
401  
402  
403  
404  
405  
406  
407  
408  
409  
410  
411  
412  
413  
414  
415  
416  
417  
418  
419  
420  
421  
422  
423  
424  
425  
426  
427  
428  
429  
430  
431  
432  
433  
434  
435  
436  
437  
438  
439  
440  
441  
442  
443  
444  
445  
446  
447  
448  
449  
450  
451  
452  
453  
454  
455  
456  
457  
458  
459  
460  
461  
462  
463  
464  
465  
466  
467  
468  
469  
470  
471  
472  
473  
474  
475  
476  
477  
478  
479  
480  
481  
482  
483  
484  
485  
486  
487  
488  
489  
490  
491  
492  
493  
494  
495  
496  
497  
498  
499  
500  
501  
502  
503  
504  
505  
506  
507  
508  
509  
510  
511  
512  
513  
514  
515  
516  
517  
518  
519  
520  
521  
522  
523  
524  
525  
526  
527  
528  
529  
530  
531  
532  
533  
534  
535  
536  
537  
538  
539  
540  
541  
542  
543  
544  
545  
546  
547  
548  
549  
550  
551  
552  
553  
554  
555  
556  
557  
558  
559  
560  
561  
562  
563  
564  
565  
566  
567  
568  
569  
570  
571  
572  
573  
574  
575  
576  
577  
578  
579  
580  
581  
582  
583  
584  
585  
586  
587  
588  
589  
590  
591  
592  
593  
594  
595  
596  
597  
598  
599  
600  
601  
602  
603  
604  
605  
606  
607  
608  
609  
610  
611  
612  
613  
614  
615  
616  
617  
618  
619  
620  
621  
622  
623  
624  
625  
626  
627  
628  
629  
630  
631  
632  
633  
634  
635  
636  
637  
638  
639  
640  
641  
642  
643  
644  
645  
646  
647  
648  
649  
650  
651  
652  
653  
654  
655  
656  
657  
658  
659  
660  
661  
662  
663  
664  
665  
666  
667  
668  
669  
670  
671  
672  
673  
674  
675  
676  
677  
678  
679  
680  
681  
682  
683  
684  
685  
686  
687  
688  
689  
690  
691  
692  
693  
694  
695  
696  
697  
698  
699  
700  
701  
702  
703  
704  
705  
706  
707  
708  
709  
710  
711  
712  
713  
714  
715  
716  
717  
718  
719  
720  
721  
722  
723  
724  
725  
726  
727  
728  
729  
730  
731  
732  
733  
734  
735  
736  
737  
738  
739  
740  
741  
742  
743  
744  
745  
746  
747  
748  
749  
750  
751  
752  
753  
754  
755  
756  
757  
758  
759  
760  
761  
762  
763  
764  
765  
766  
767  
768  
769  
770  
771  
772  
773  
774  
775  
776  
777  
778  
779  
780  
781  
782  
783  
784  
785  
786  
787  
788  
789  
790  
791  
792  
793  
794  
795  
796  
797  
798  
799  
800  
801  
802  
803  
804  
805  
806  
807  
808  
809  
810  
811  
812  
813  
814  
815  
816  
817  
818  
819  
820  
821  
822  
823  
824  
825  
826  
827  
828  
829  
830  
831  
832  
833  
834  
835  
836  
837  
838  
839  
840  
84

- ۲۵ -

○ - ۲۶ -

○ - ۲۷ -

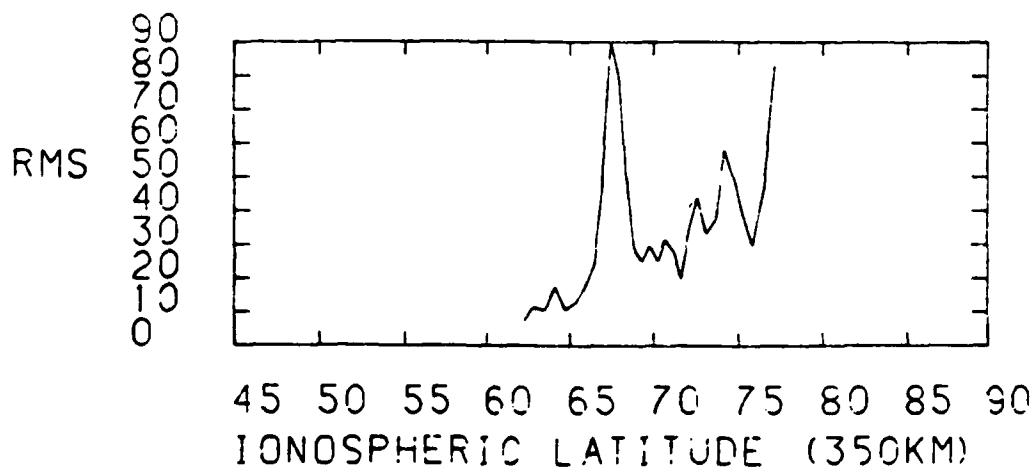
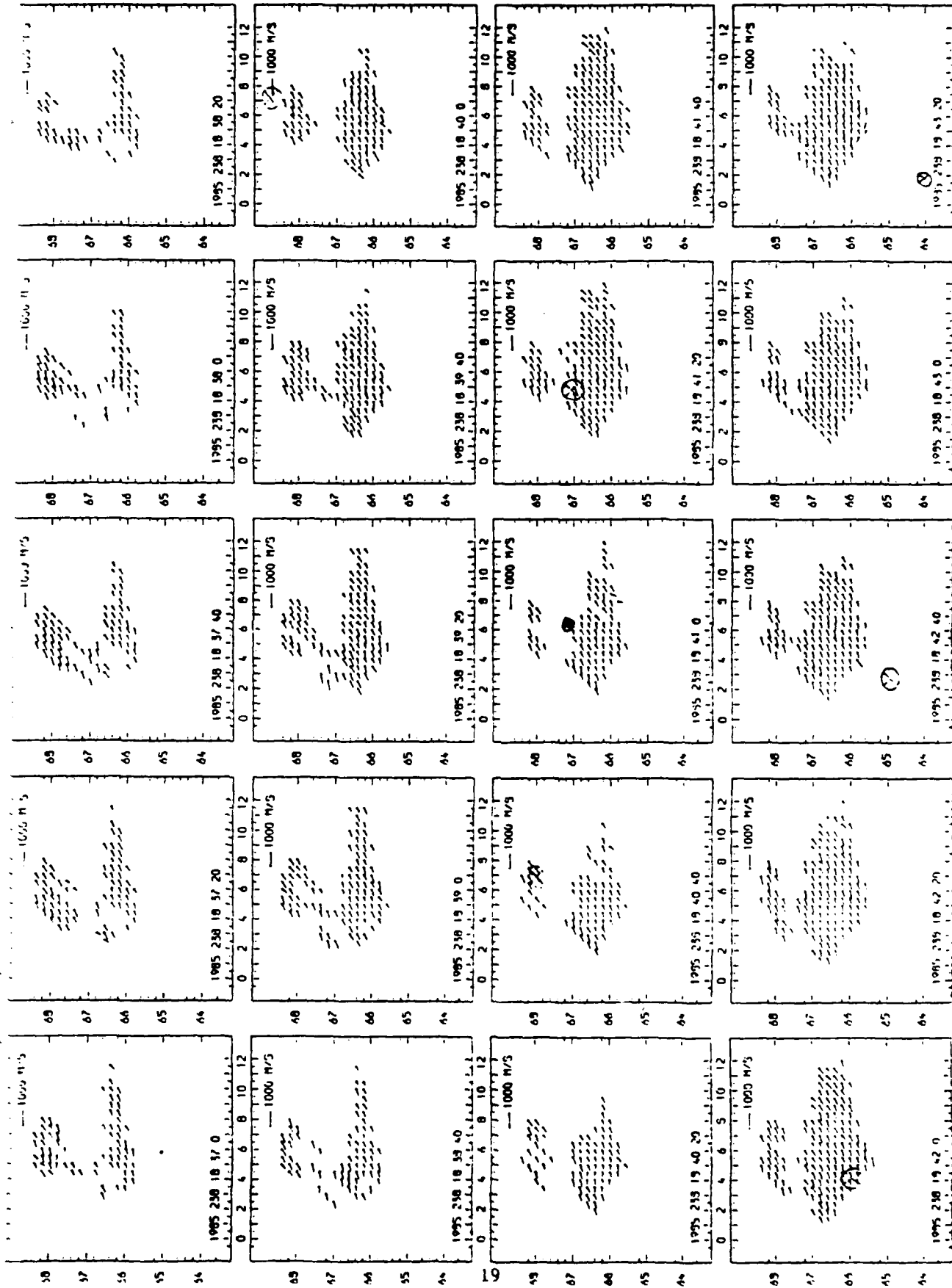


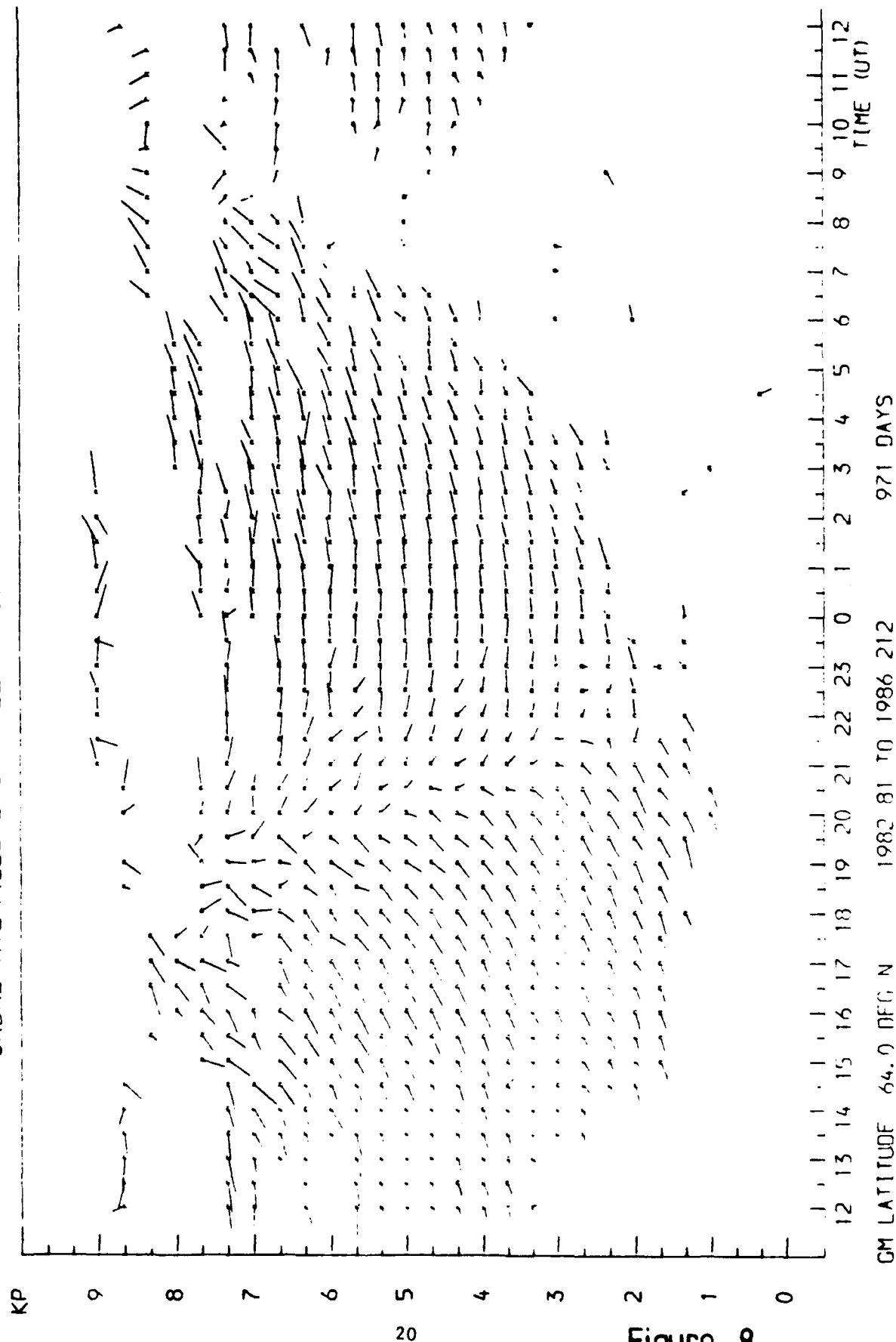
Figure 6

Figure 7



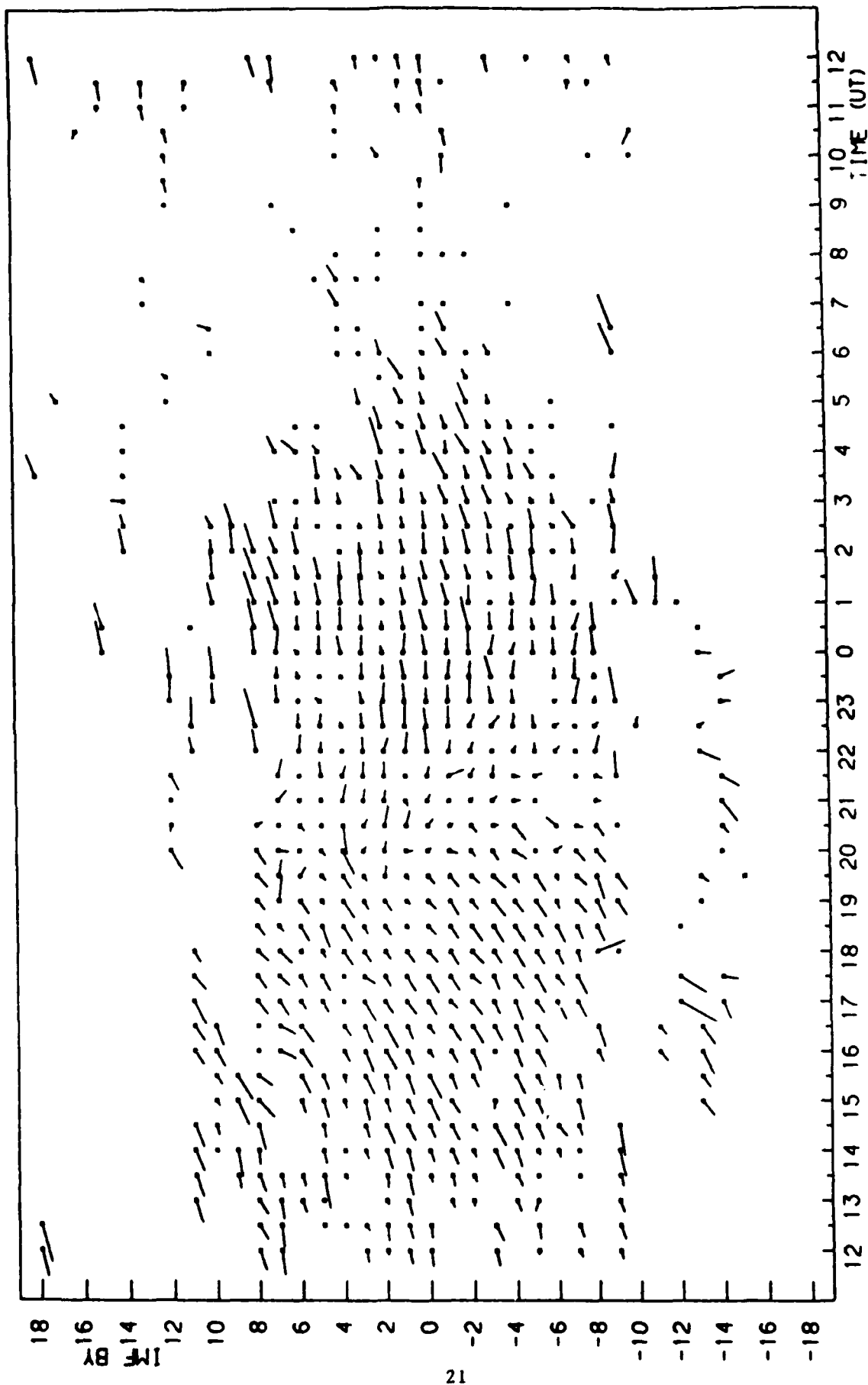
1000 M/S

# SABRE AVERAGED DRIFT VELOCITIES



# SABRE AVERAGED DRIFT VELOCITIES

1000 M/S



902.00 HOURS DATA

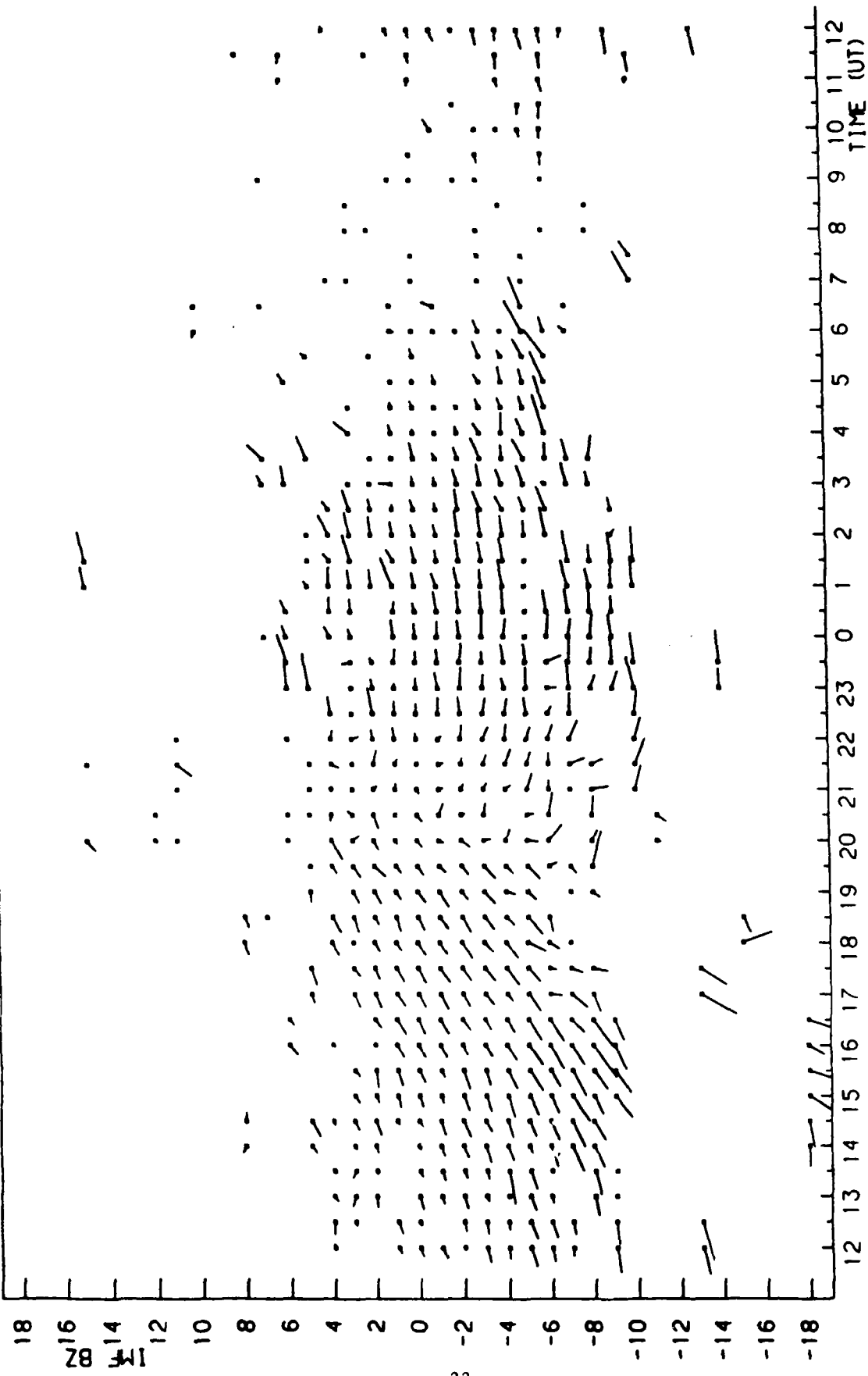
1982 81 TO 1984 67

GM LATITUDE 64.0 DEG N

TIME (UT)

# SABRE AVERAGED DRIFT VELOCITIES

1000 M/S



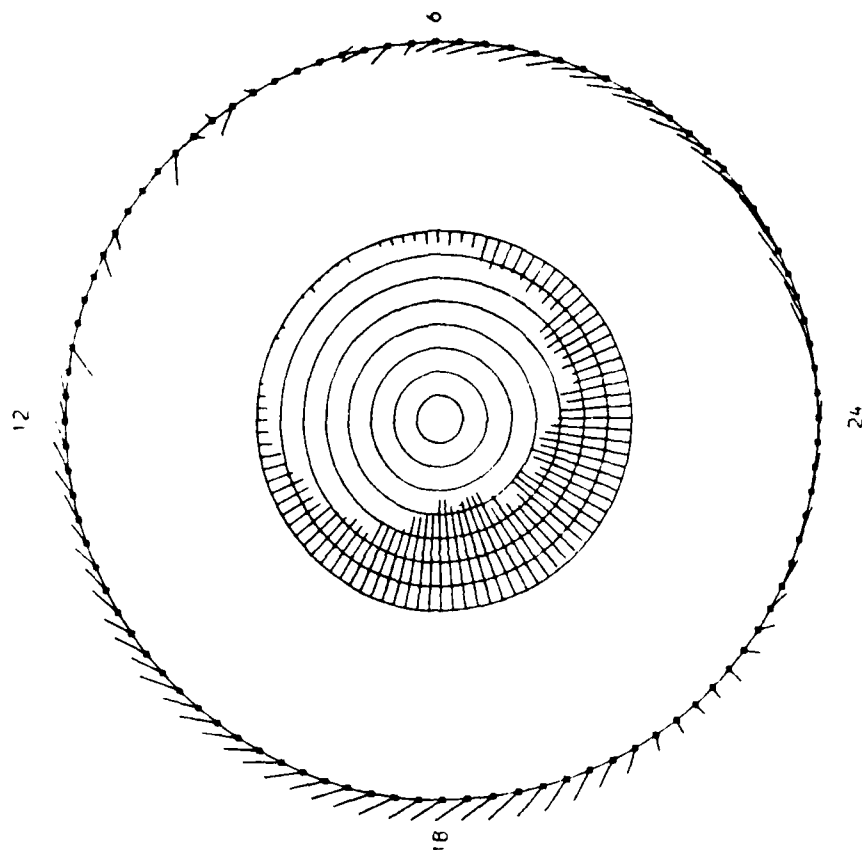
902.00 HOURS DATA

1982 81 TO 1984 67

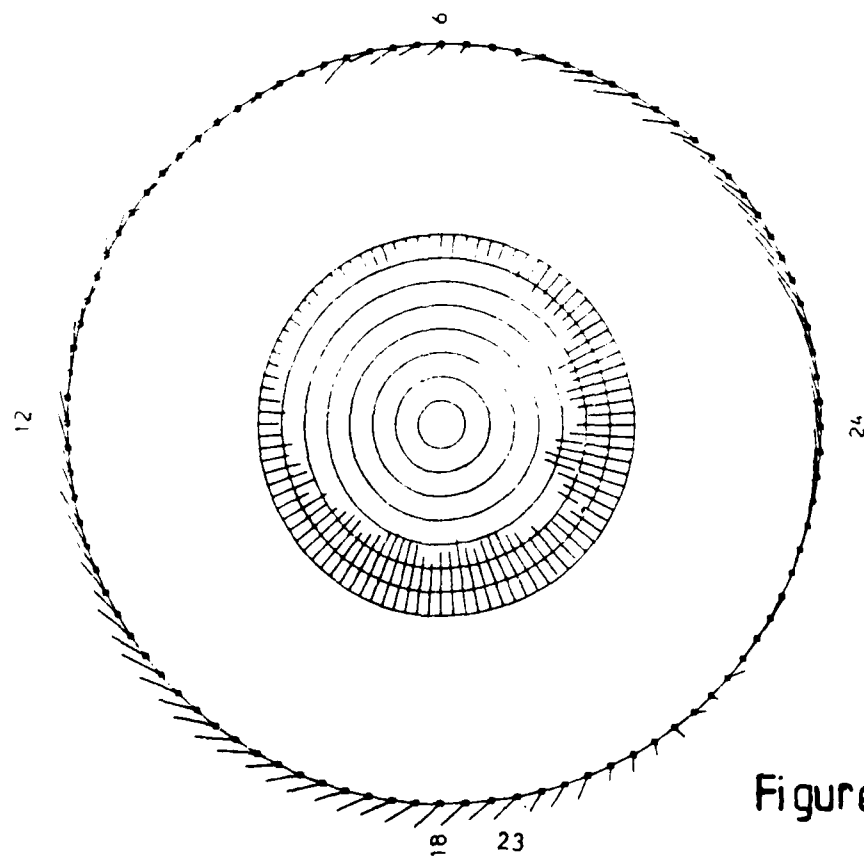
CM LATITUDE 64.0 DEC N

Figure 10



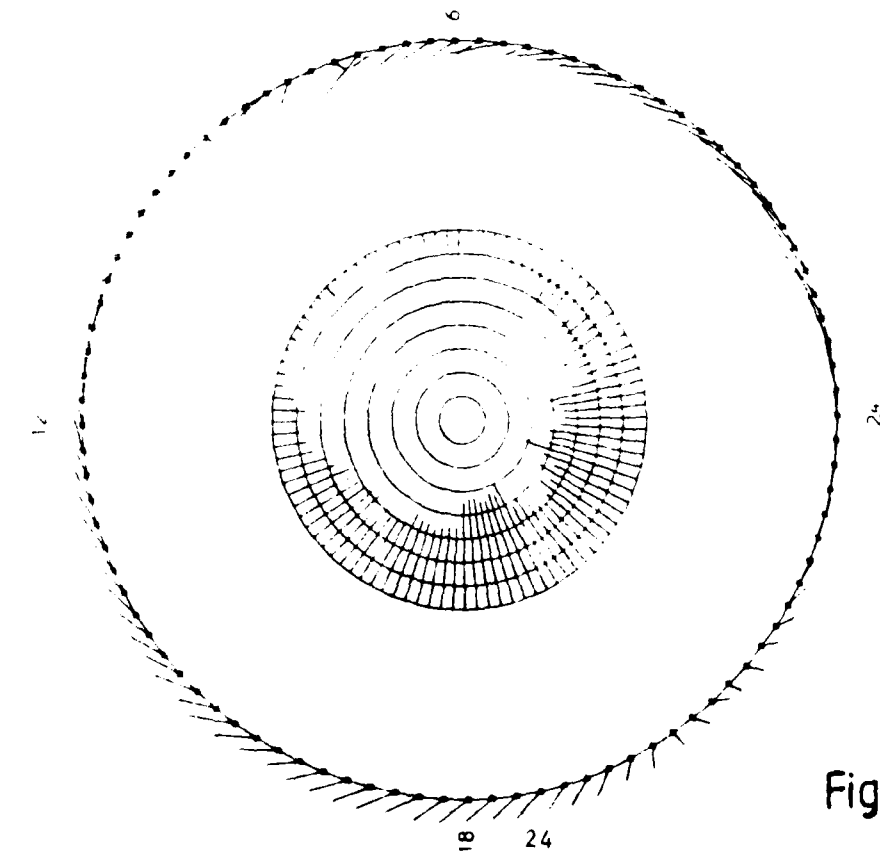


BY < 0.0 ALL BZ  
488.25 HOURS DATA

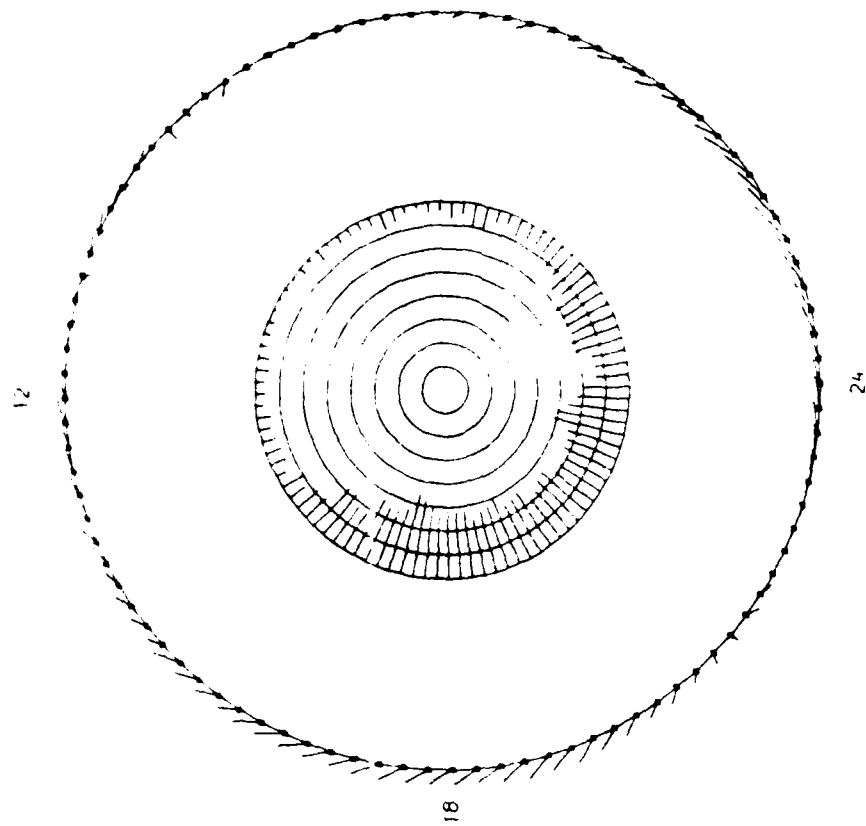


BY > 0.0 ALL BZ  
420.50 HOURS DATA

Figure 11



ALL BY  
565.00 HOURS DATA  
B7 > 0.0



ALL BY  
351.25 HOURS DATA  
B7 > 0.0

Figure 12

ATE  
MED  
8